33ND INTERNATIONAL COSMIC RAY CONFERENCE, RIO DE JANEIRO 2013
THE ASTROPARTICLE PHYSICS CONFERENCE

Expected Performance of CALET as a High Energy Gamma Ray Observatory

MASAKI MORI[1] FOR THE CALET COLLABORATION.

[1] *Department of Physical Sciences, Ritsumeikan University, Kusatsu, Shiga 525-8577, Japan*

morim@fc.ritsumei.ac.jp

Abstract: The CALorimeteric Electron Telescope (CALET) is a Japanese-led international mission being developed as part of the utilization plan for the International Space Station (ISS). CALET will be launched by an H-II B rocket utilizing the Japanese developed HTV (H-II Transfer Vehicle) in 2014. It will measure high-energy electrons, cosmic-rays as well as gamma rays above 10 GeV to more than 10 TeV with high accuracy. In this paper, the expected performance of CALET as a high-energy gamma-ray observatory is discussed based on a Monte Carlo simulation.

Keywords: CALET, gamma-rays, observation.

1 Introduction

The CALorimeteric Electron Telescope (CALET) is a Japanese-led international mission being developed as part of the utilization plan for the International Space Station (ISS). CALET will be launched by an H-II B rocket utilizing the Japanese developed HTV (H-II Transfer Vehicle) in 2014. It will measure high-energy electrons, cosmic rays as well as gamma rays above 10 GeV to about 10 TeV with high accuracy [1].

The CALET detector will always watch the zenithal direction on the ISS frame, but the ISS orbit makes the CALET an all-sky monitor of high-energy gamma rays. The survey of the variable gamma-ray sky with CALET above 10 GeV enables us to study the high-energy universe up to higher energies and with a better energy resolution than Fermi-LAT.

In this paper, the expected performance of CALET as a high-energy gamma-ray observatory is discussed based on a Monte Carlo simulation. The instrument response functions (IRF), such as effective area, energy and angular resolution, are derived. Expected scientific results of CALET as a gamma-ray observatory will be presented in the accompanying paper [2]. Expected performance of CALET for dark matter search will be presented in a separate paper [3].

2 Simulation

2.1 The CALET detector

The schematic concept of CALET is shown in Fig.1. It consists of Charge Detector (CHD), Imaging Calorimeter (IMC), and Total Absorption Calorimeter (TASC) [1]. CHD is made of a set of X- and Y-direction array of 14 plastic scintillator strips (32 mm $\times$ 10 mm $\times$ 448 mm). IMC is composed of 8 layers of X- and Y-direction array of 448 scintillation fibers (SciFi, 1 mm $\times$ 1 mm $\times$ 448 mm) separated by tungsten plates, whose upper five plates have thickness of$0.2X_0$ (radiation length) and lower two have $1.0X_0$, in total of $3X_0$ thickness. (In the following these 8 layers are called L0–L7, respectively.) TASC is made of 6 layers of X- and Y-array of 16 PWO scintillation crystals (19 mm $\times$ 20 mm $\times$ 326 mm) in total of 27 X_0 thickness. These thick layers of material enable CALET to detect gamma rays up to 10 TeV energies with high accuracy.

For gamma-ray observation, we mainly use the 'high-energy trigger' for showering particles above 10 GeV, in which events are triggered in combination of IMC (signal sum of SciFi one X and one Y layers) and TASC (signal sum of the top layer).

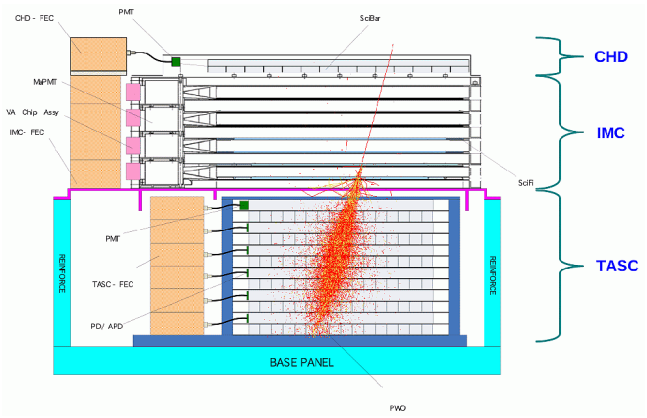

Figure 1: A schematic concept of CALET. (Note the event shown here is a 1-TeV electron.)

2.2 Monte Carlo calculation

The Monte Carlo simulation code, EPICS, has been used to estimate the expected performance of CALET which takes account of the detector configuration, as descibed in Ref.[4]. Using the similar procedure, the effectuve area, angular resolution and energy resolution of CALET for gamma-ray observation are estimated as described in the next section.

2.3 Event reconstruction

The event reconstruction algorithm for gamma rays used here proceeds as follows:

1. *Estimation of shower axis using IMC.*
   The center-of-gravity of signals in the lowest two layers of IMC are calculated and the shower axis is

determined. Then the similar procedure is repeated including the next layer of IMC, and this process is repeated as long as the signal in the next layer is present. Thus the accuracy of track reconstruction is related to the number of hit layers of IMC, which reflects the position of conversion of gamma rays into electron-positron pairs.

2. *Check of the axis with TASC.*
The distribution of signals in the third and fourth layers of TASC should be consistent with the assumed shower axis. Otherwise the event is discarded. Signals in TASC are the measure of gamma-ray energies.

3. *Separation from electrons using IMC/CHD.*
We accept only gamma rays which interact after the first layer of IMC, so there should be no signal in CHD and the top layer of IMC. In practice, we require those signals should be less than a half of the signal caused by minimum ionizing particles.

Since the primary objective of CALET is to detect cosmic-ray electrons among the 'sea' of background hadrons, the proton survival probability in electron samples to be achieved is at the level of 10^{-5} while maintaining 80% detection efficiency for electrons [1, 4]. The same discrimination scheme can be applied to gamma-ray samples. Identification of gamma-rays from electrons is executed in the step 3 above. In the present algorithm we misidentify less than one electron from 10,000 gamma rays: this misidentification probability will be reduced by fine tuning of parameters in the reconstruction procedure.

2.4 Event classification

The IRF depends on the event geometry and the position of electron-postron pair conversion of gamma-rays.

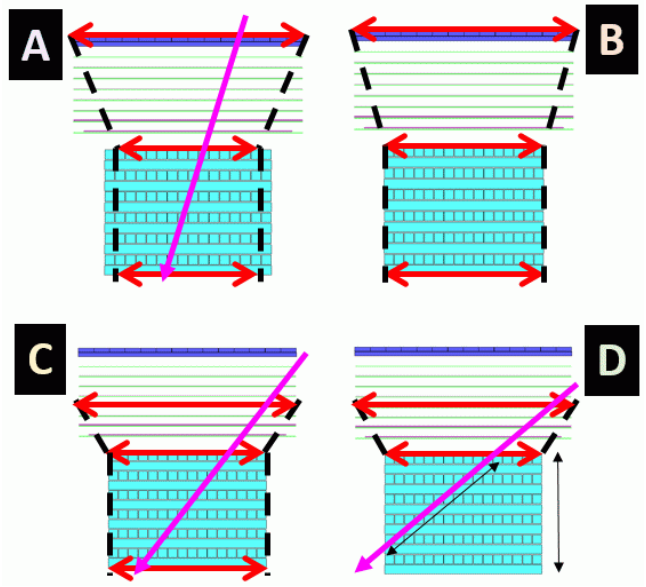

Figure 2: Schematics of 4 types of CALET gamma-ray event geometry requirements.

Fig.2 shows schematically the four track geometry requirements for classifying gamma-ray candidate events. The geometry A requires the track should pass through CHD and 2 cm (width of a PWO unit) inside the top and the bottom layers of TASC. This is the most severe requirement and would yield the best performance. The geometry B requires similar condition, but any hit position in the top and the bottom layers of TASC are allowed. The geometry C requires the track should pass through the fourth layer of IMC, and the top and bottom layers of TASC. The geometry D requires the track should pass through the fourth layer of IMC and the top layer of TASC, plus the track length in TASC should be more than $27X_0$. This is the loosest but the largest area option.

As for the postion of conversion, we mainly assume two cases: one is conversion in upper four (thin) layers (L1–L4) of tungsten plates in IMC and the other is conversion in any layers including the lowest thin layer (L5) and lower two thick layers (L6 and L7) of IMC. Because of the longer baseline and more tracking points, charged particle tracks are more accurately reconstructed when gamma-rays are converted into electron-positron pairs in the upper layers of IMC.

Different options could be used in case by case for scientific merits, e.g. the best performance option could be applied for high resolution study of spatially resolved sources, and the large-area option could be applied for high-latitude faint blazars. (See ref.[2] for more discussion.)

3 Results

3.1 Effective area

The results on effective area is shown in Fig.3 for normal incidence. They are plotted for four cases, i.e., the combination of position of conversion (upper layers [solid line] or full layers [dashed line]) and two track geometries (A or D: area is always larger for the geometry D than A). The effective area is almost constant above 12 GeV, and reaches above 600 cm^2 for the geometry D and full layers,

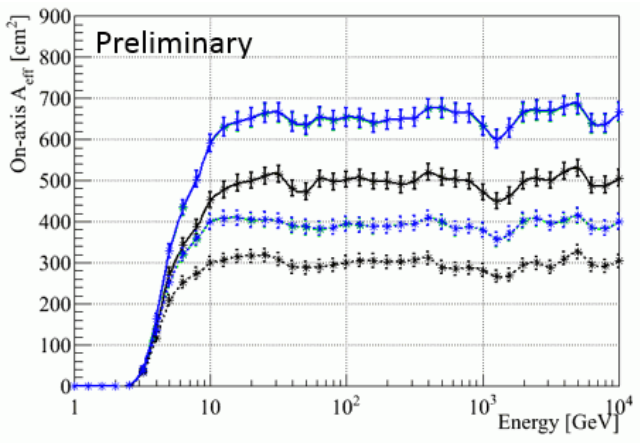

Figure 3: CALET effective area for gamma rays. Solid and dashed lines correspond to conversion in full layers and upper (thin) layers, respectively, and two lines each for the geometries D and A. (The effective area is always larger for the geometry D than for A.)

3.2 Energy resolution

Fig.4 shows the energy resoltion for gamma rays of normal incidence. Here the results for the tightest requirement, geometry A, and the loosest requirement, geometry D, are assumed. In this case the position of pair conversion of gamma rays influence little, since the energy is estimated using TASC signals. The energy resolution is 3% at 10 GeV even if the loosest geometry is used. The resolution above 100 GeV becomes worse slowly as energy increases, since of the number of backscattering particles inside the detector becomes significant.

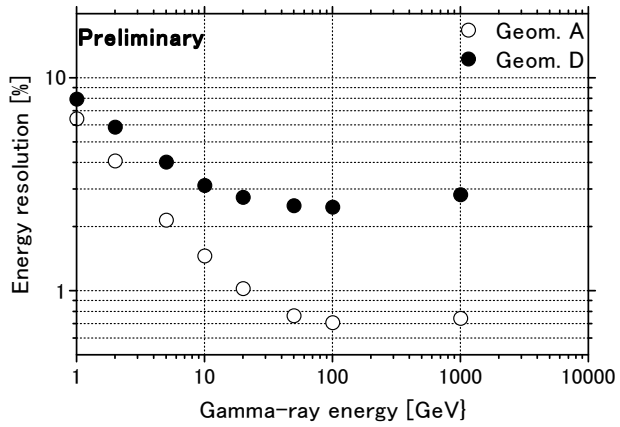

Figure 4: CALET energy resolution for gamma rays of normal incidence.

3.3 Angular resolution

Fig.4 shows the angular resoltion for gamma rays, which is defined as the half-cone angle containing more than 68% of events, of normal incidence. It is rather heavily dependent on the position of pair conversion, so the five plots are given for different requirements: the best resolution is expected for conversion in L1, then it becomes worse when we include events converted in lower layers ('$\leq$L2' means conversion in L1 or L2, and so on.) The total angular resolution is 0.35° at 10 GeV and about 0.2° at 100 GeV, then it gradually becomes worse as energy increases, due to the similar reason to energy resolution.

4 Conclusion

The perfomance of the CALET detector to be launched and installed on ISS in 2014 has been evaluated for gamma-ray observation with a Monte Calro simulation, and IRFs are given. Gamma-ray performance parameters of CALET are summarized in Table 1 in comparison with other missions. Expected scientific results from gamma-ray observataions with this performance will be described in the accompanying paper [2].

Thus, CALET will be a good all-sky monitor of gamma rays above 10 GeV during its mission of 5 years. Particularly, with its good energy resolution, CALET can explore narrow-line feature in the gamma-ray spectrum

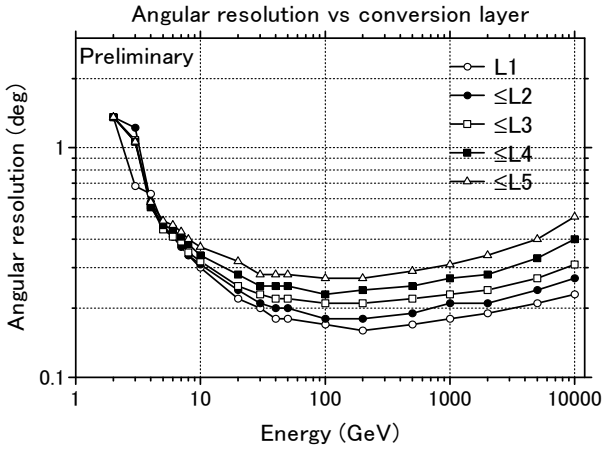

Figure 5: CALET angular resoltuion for gamma rays of normal incidence. The curve 'L1' is for gamma-rays converted in L1, '$\leq$L2' is those in L1 or L2, and so on.

which might be caused by dark matter annihilation (see [3]).

Acknowledgment: This effort is supported by NASA in the United States, by JAXA in Japan and ASI in Italy. Also it is partly supported by the Grant-in-Aid from the Ministry of Education, Culture, Sports, Science and Technology (MEXT) of Japan, No. 22540315 (MM). e acknowledge contibutions to this work by Mr. Yuki Mori.

References

[1] S. Torii for the CALET Collaboration, "CALET Mission for Exploring the High Energy Universe" (in Japanese), IEEJ Transactions on Fundamentals and Materials, 132, 8, 603-608 (2012); S. Torii et al., "The Calorimetric Electron Telescope (CALET) for High Energy Astroparticle Physics on the International Space Station", Paper ID 245 in this conference.
[2] A. Moiseev et al., "CALET perspectives in high-energy gamma-ray observations", Paper ID 627 in this conference.
[3] K. Yoshida et al., "Dark Matter Search with CALET", Paper ID 735 in this conference.
[4] Y. Akaike et al., "Expected CALET Telescope Performance from Monte Carlo Simulations", Proc. 32nd ICRC (Beijing), Vol.6, pp.371–374 (2011); Y. Akaike et al., "CALET observational performance expected by CERN beam test", Paper ID 726 in this conference.
[5] CGRO Science Support Center, http://heasarc.gsfc.nasa.gov/docs/cgro/egret/egret_tech.html
[6] M. Tavani et al., "The AGILE Mission", Astron. Astrophys. 502, 995–1013 (2009)
[7] W.B. Atwood et al., "The Large Area Telescope on the Fermi Gamma-Ray Space Telescope Mission", Astrophys. J. 697, 1071–1102 (2009); http://www.slac.stanford.edu/exp/glast/groups/canda/lat_Performance.htm

	CGRO/EGRET [5]	AGILE [6]	Fermi/LAT [7]	CALET
Energy range	30 MeV–30 GeV	100 MeV– 50 GeV	20 MeV–300 GeV	4 GeV–10 TeV
Effective area	1500 cm^2	600 cm^2 (100 MeV)	6700 cm^2 (1 GeV) 7600 cm^2 (10 GeV)	600 cm^2 (10 GeV)
Field-of-view	0.5 sr	2.5 sr	2.5 sr	2 sr
Geometrical factor			1.7 m^2sr (1 GeV) 2.0 m^2sr (10 GeV)	1100 cm^2sr (10 GeV)
Energy resolution	20% (200–3000 MeV)	100% (400 MeV)	9% (1 GeV) 8% (10 GeV)	3% (10 GeV)
Angular resolution	5.8° (100 MeV)	3.5° (100 MeV) 1.2° (400 MeV)	0.9° (1 GeV) 0.25° (10 GeV)	0.35° (10 GeV)
Deadtime	100 ms	100–200 μs	26.5 μs	2 ms
Pointing accuracy	$15'$	6–12’	$0.5'$	$6'$
Point source sensitivity	$\sim 1\times10^{-7}$cm^{-2}s^{-1}	$\sim 3\times10^{-7}$cm^{-2}s^{-1}	3×10^{-9}cm^{-2}s^{-1}	8×10^{-9}cm^{-2}s^{-1}
Observation period	1991–2000	2007–	2008–	2014 (planned)–

Table 1: Comparison of high-energy gamma-ray observatories.